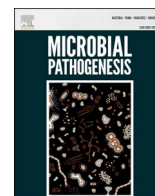




Since January 2020 Elsevier has created a COVID-19 resource centre with free information in English and Mandarin on the novel coronavirus COVID-19. The COVID-19 resource centre is hosted on Elsevier Connect, the company's public news and information website.

Elsevier hereby grants permission to make all its COVID-19-related research that is available on the COVID-19 resource centre - including this research content - immediately available in PubMed Central and other publicly funded repositories, such as the WHO COVID database with rights for unrestricted research re-use and analyses in any form or by any means with acknowledgement of the original source. These permissions are granted for free by Elsevier for as long as the COVID-19 resource centre remains active.



Structure-based screening of natural product libraries in search of potential antiviral drug-leads as first-line treatment to COVID-19 infection

S.J. Aditya Rao^{*}, Nandini P. Shetty

Plant Cell Biotechnology Department, CSIR-Central Food Technological Research Institute, Mysore, 570020, Karnataka, India

ARTICLE INFO

Keywords:

Drug design
Synthetic drugs
Structural diversity
SARS-CoV-2
Medicinal chemistry

ABSTRACT

The study focuses on identifying and screening natural products (NPs) based on their structural similarities with chemical drugs followed by their possible use in first-line treatment to COVID-19 infection. In the present study, the in-house natural product libraries, consisting of 26,311 structures, were screened against potential targets of SARS-CoV-2 based on their structural similarities with the prescribed chemical drugs. The comparison was based on molecular properties, 2 and 3-dimensional structural similarities, activity cliffs, and core fragments of NPs with chemical drugs. The screened NPs were evaluated for their therapeutic effects based on their predicted *in-silico* pharmacokinetic and pharmacodynamics properties, binding interactions with the appropriate targets, and structural stability of the bound complex using molecular dynamics simulations. The study yielded NPs with significant structural similarities to synthetic drugs currently used to treat COVID-19 infections. The study proposes the probable biological action of the selected NPs as Anti-retroviral protease inhibitors, RNA-dependent RNA polymerase inhibitors, and viral entry inhibitors.

1. Introduction

Viral infections play an important role in human diseases, and their regular outbreaks repeatedly underlined the need for their prevention in safeguarding public health [1]. The recent outbreak of COVID-19 disease was declared a 'public health emergency of international concern' by World Health Organization (WHO) in view of its severity [2]. The Coronavirus disease (COVID-19), previously known as '2019 novel coronavirus' or '2019-nCoV', is an infectious disease caused by a newly discovered coronavirus; severe acute respiratory syndrome coronavirus 2 or SARS-CoV-2 [3]. The SARS-CoV-2 is a member of the *Coronavirinae* family belonging to the *Betacoronavirus* genus [4]. Structurally it is spherical or pleomorphic in shape, with a diameter of about 60–140 nm. All ages are susceptible to COVID-19 infection, and its clinical manifestations range from asymptomatic to mild to severe and even to death depending on the underlying health conditions of individuals [5,6]. The most commonly reported symptoms are fever, chills, headache, body aches, dry cough, fatigue, pneumonia, and complicated dyspnea. The virus transmits from person to person via the nasal, oral, eye, and mucosal secretions of the infected patient and direct transmission through the inhalation of droplets released during the patient's cough or sneeze [7, 8].

Fig. 1 describes some of the most widely used vaccines currently developed against COVID-19. The other potential treatment strategies include inhibition of RNA-Dependent RNA Polymerase activity, viral protease inhibition, viral entry inhibition, immune modulation, monoclonal antibodies, janus kinase inhibitors, nutritional supplements, and conventional plasma therapy (Table S1) [9]. The developmental status of different antiviral drugs to treat COVID-19 conditions is shown in Fig. 2.

Natural products and traditional medicines have been serving as the greatest source for modern drug discovery. Their derivatives have been recognized for many years as the source of therapeutic potential and structural diversity. There are over 200,000 compounds reported in the scientific literature. NPs are more often structurally complex, with well-organized structure and steric properties offering efficacy, efficiency, and selectivity of molecular targets [10]. However, their utilization on many health conditions is well documented; it is in the hands of existing traditional practitioners and herbologists to define their applications for newly emerging diseases. The biological activities reported from different plant extracts often narrow down to pre-reported molecules rather than novel compounds [11], creating a real challenge to medicinal chemists. In this avenue, the search for new therapeutic molecules is the need of the hour to combat new health challenges.

^{*} Corresponding author.

E-mail address: adityaraosj@gmail.com (S.J.A. Rao).

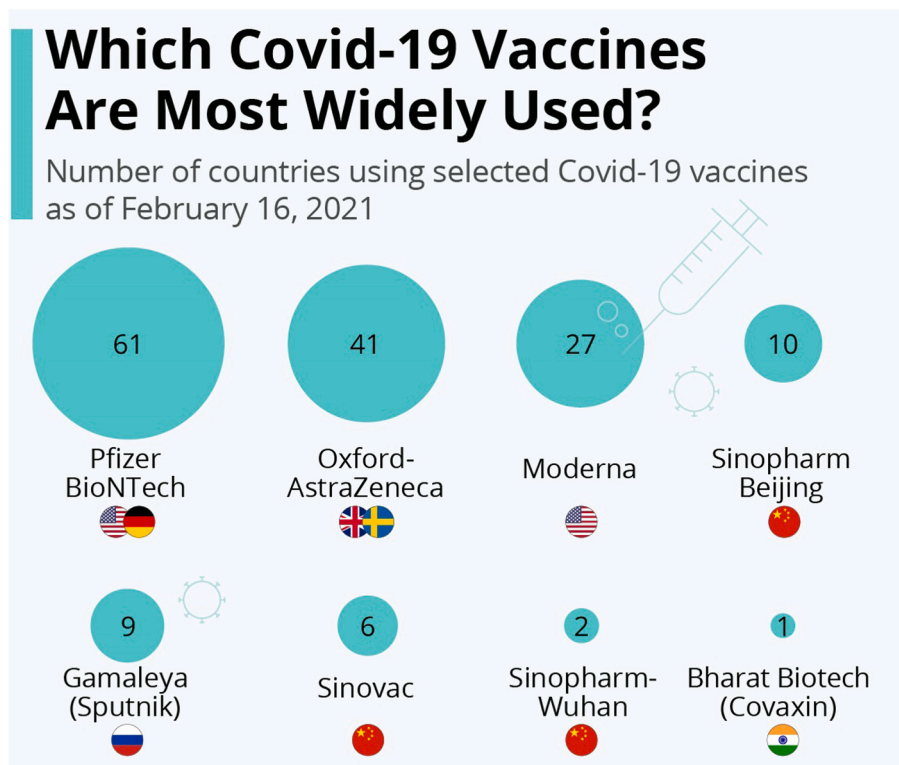


Fig. 1. Most widely used vaccines currently developed against COVID-19.

The biological activity of any molecule is attributed to its structural arrangements. If two molecules have a similar structure, they will probably have a similar biological effect [12–14] (Fig. 3). The computational chemists successfully exploit this principle for the construction of diverse compound libraries and select compounds for high-throughput screening experiments [12]. Computational advancements with the introduction of parallel processing clusters, cloud-based computing, and highly effective graphical processing units (GPUs), tremendous success has been achieved in the field of modern drug discovery [15]. The knowledge of natural products and ligands, earlier used as starting points for drug discovery, has greatly influenced computational biology techniques [16]. These advancements have been speeded up by the creation of new algorithms for more accurate predictions, simulations, and interpretations [17–22]. The extensive molecular dynamics (MD) simulations can provide insights into the host-virus interactions, disease spread, and possible regulative/preventive mechanisms [23]. In this avenue, the present study proceeds to exploit these developments to identify natural products as potential drug leads targeting some of the most widely used antiviral drugs currently being used against SARS-CoV-2. The identified molecules envisage to be potential drug leads and, with critical screening and trials, could be used in the first-line treatment for COVID-19 infections.

2. Material and method

2.1. Dataset collection and library construction

An in-house natural product library consisting of 26,311 natural product structures was constructed using natural products information from different databases like Dr. Duke's database (<https://phytochem.nal.usda.gov/phytochem/search>) [24], Phytochemical Interactions Database (<http://www.genome.jp/db/picdb>), and Natural product activity and species source database (NPASS) (<http://bidd.group/NPASS/index.php>) [25]. The plant's secondary metabolites are classified into various classes according to their chemical structures [26]. Their

classification as phenolics, alkaloids, Flavonoids, Tannins, Coumarins, terpenes, Lignans, etc., with polyphenols further classified into flavans, flavones, and isoflavonoids are of particular interest to medicinal chemists due to their diverse therapeutic effects [27,28]. Therefore, the polyphenols from the natural product library were further categorized as flavans (339), flavones (193), and isoflavonoids (457), and the rest of the molecules as a general group. The broad-spectrum antiviral drugs currently under investigation to treat COVID-19 conditions were collected from the drugvirus.info server (<https://drugvirus.info>). For comparison, the small molecule synthetic drugs were categorized into molecules present in Pubchem COVID-19 portal (306) [29] (<https://pubchem.ncbi.nlm.nih.gov/#query=covid-19>), and molecules present at different stages of clinical trials (138) (As of 31st August 2020) based on the available information from ClinicalTrials.gov database [30] (<https://www.clinicaltrials.gov/ct2/home>). Further, the study was extended to compare the most promising investigational drugs like Remdesivir, Arbidol, Lopinavir, and Ritonavir. The top 10 structures with structurally most similar to investigational drugs were selected for *in-silico* PK/PD analysis and HTVS (high throughput virtual screening) studies.

2.2. Structure-based screening of natural products

The non-redundant natural product libraries were compared against chemical drugs currently under prescription/study to treat COVID-19 infection. The comparison was based on 2 and 3-dimensional structural similarities, activity cliffs (ACs), and core fragments (CFs). The structural similarities were assessed based on the number of fragments that both molecules have to the number of fragments found in any two structures [31]. The structural scaffolds (SSs) were analyzed based on plane ring system to determine the sub-structures. ACs, CFs, and SSs were determined employing Osiris DataWarrior V.4.4.3 software [31].

a Pharmacophore based comparison of natural products with their synthetic drugs counterparts:

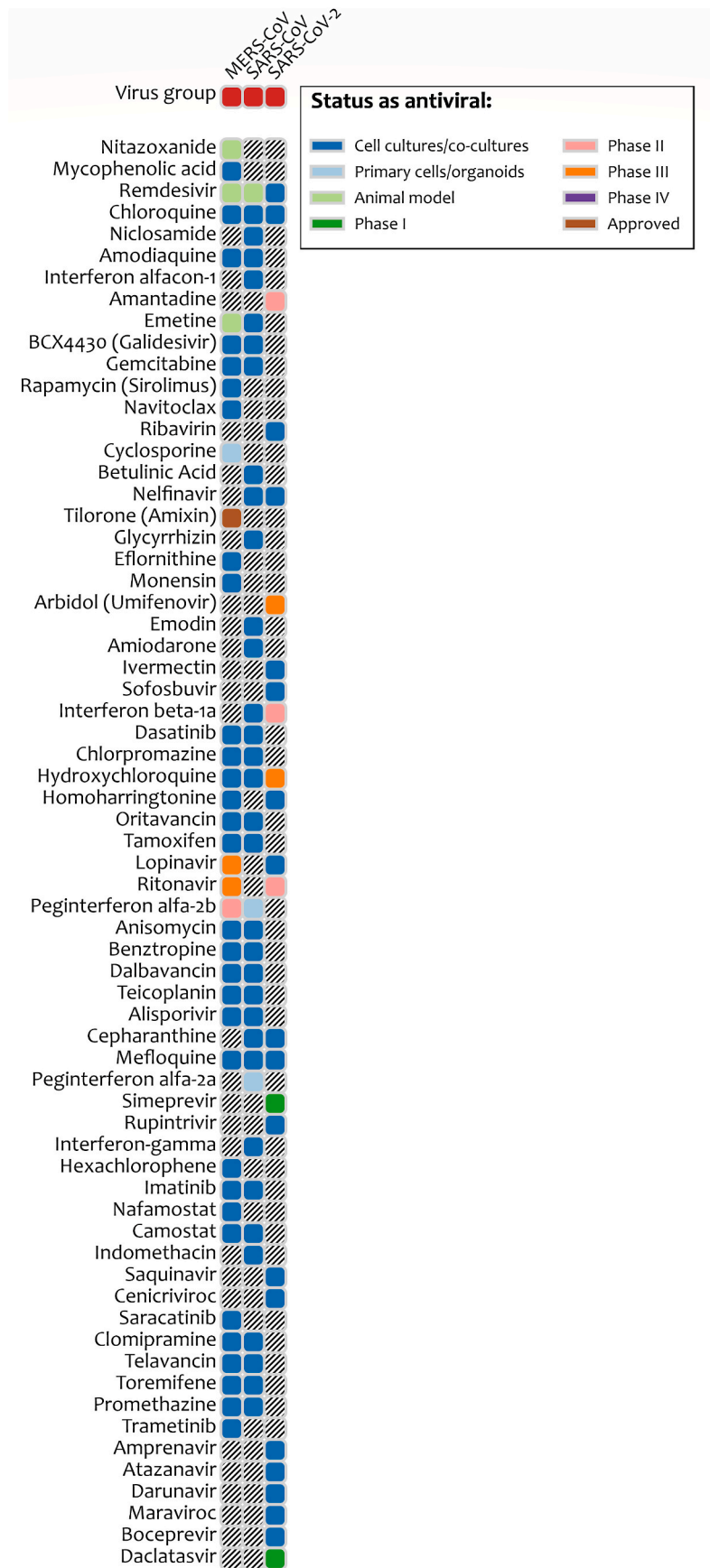


Fig. 2. The broad-spectrum antiviral drugs currently being investigated to treat the COVID-19 condition.

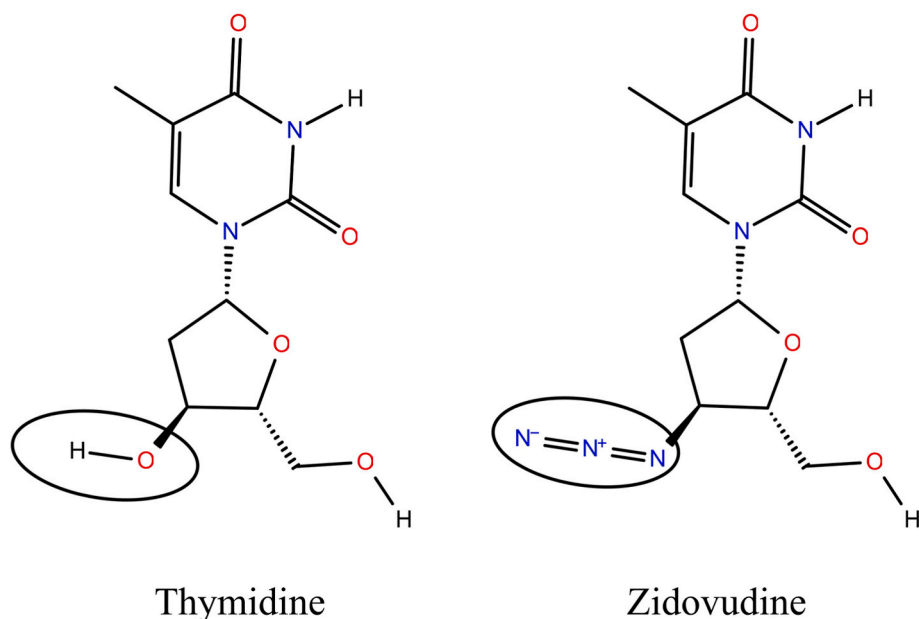


Fig. 3. A comparison describing the structural similarities with variations highlighted inside the ellipse between thymidine, a naturally occurring nucleotide base, and zidovudine, a synthetic drug used to treat HIV patients. Structurally both the molecules share >93% identity.

To find structurally similar compounds rather than compounds sharing a common sub-structure, core fragment-based SAR analysis was performed by considering the most central ring structure. The similarities between the fragments were assessed based on the number of fragments that both molecules have in common, divided by the number of fragments being found in any of the two structures [31–33]. The structures were further analyzed for structural scaffolds based on plane ring system to determine the substructures and to define the similarity cut-off during the structure comparison. The molecular properties, activity cliff, core fragments, and structural scaffolds were predicted using Osiris DataWarrior V.4.4.3 software [31,34].

b Similarity score cut-off limit:

Natural products exist in many of their stable analogs forms in nature. Even with minor structural variations, the analogous forms of natural products can exert unique biological effects [35]. Therefore, there was a need to set an appropriate limit to filter natural products and their analogous structures. Due to their complex structures, at higher cut-off limits, such derivatives are expected to exclude, while at lower cut-off limits, the analogous structures become inclusive (Table S2). By considering such variations, a similarity cut-off limit of 60% was fixed for the comparison [34].

2.3. Molecular properties based PK/PD analysis

Natural products are the major source of oral drugs ‘beyond Lipinski’s rule of five’ [36–38]. The drug-likeness assessment, pharmacokinetic (PK), and pharmacodynamics (PD) of NPs were determined based on their molecular properties like molecular weight, cLogP, hydrogen atom donors, hydrogen atom acceptors, and rotatable hydrogen bonds. These properties are used as filtering parameters to estimate the oral bioavailability, solubility, and permeability of new drug candidates [36,38,39]. The natural products obtained from

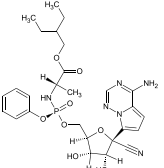
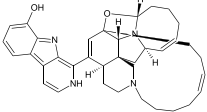
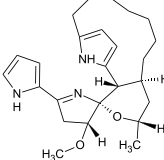
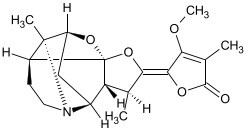
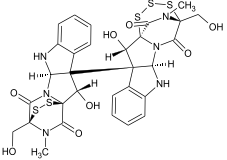
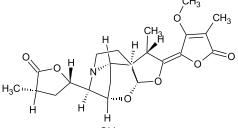
structural comparison were considered as hits for *in-silico* PK/PD assessment to analyze mutagenicity, tumorigenicity, reproductive effectiveness, irritant properties, and drug likeliness. Molecular properties were predicted using Osiris Data warrior V.4.4.3 software [31]. The admetSAR server [40] was used to predict solubility, permeability, GPCR ligand, ion channel modulator, protease inhibitor, kinase inhibitor, enzyme inhibitor, nuclear receptor inhibitor, aqueous solubility, TPSA (Topological polar surface area), blood-brain barrier penetration, human intestinal absorption, Caco-2 permeability, AMES toxicity, carcinogenicity and acute oral toxicity of the selected molecules [38,21].

2.4. Molecular interactions studies using automated docking

Automated docking was performed to deduce the binding interactions of selected natural products with appropriate target proteins. Broyden-Fletcher-Goldfarb-Shanno algorithm implemented in the AutoDockVina was employed to study proper binding modes of the selected natural products in different conformations [42]. The antiviral drugs currently being prescribed for COVID-19 first-line treatment were retrieved from the drugvirus.info server, and their action mechanisms were studied using the Inxight: Drugs database (<https://drugs.ncats.io/>) (Table S1).

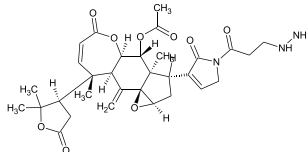
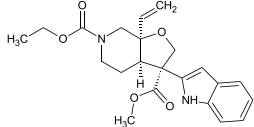
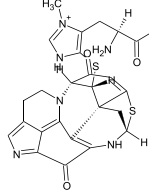
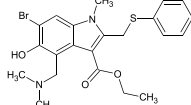
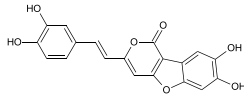
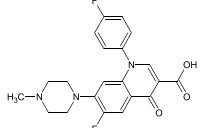
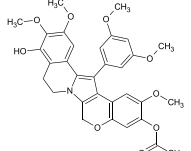
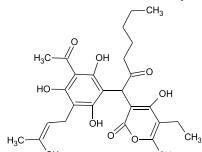
Based on the action mechanism of the standard drugs, HIV-1 protease I50V isolate, influenza virus hemagglutinin, SARS-CoV NSP12 polymerase, and HIV-1 protease A02 isolate were selected for the docking studies. The protein structures were retrieved from protein databank (<https://www.rcsb.org/>) and were prepared for docking studies. For each target, residues forming the binding site were retrieved using the PDBsum server. The antiviral drug; Lopinavir and its related natural products were docked against anti-retroviral protease inhibitor (I50V isolate) (PDB ID 3OXV), Ritonavir and its related natural products were docked against anti-retroviral protease inhibitor (A02 isolate) (PDB ID 4NJV), Remdesivir, and its related natural products were docked against anti-retroviral protease inhibitor (PDB ID 7BV2), and Arbidol and its

Table 1
Natural products (with NPASS accession) that are structurally similar to prescribed COVID-19 drugs and their similarity score.

Synthetic drug and the identified NPs	Molecular structure	Similarity score
Remdesivir		
12,28-Oxa-8-Hydroxy-Manzamine A (NPC471891)		0.7676
Marineosin A (NPC141377)		0.7558
Bis(Gorgiacerol)Amine (NPC128683)		0.8107
Methylstemofoline (NPC477986)		0.7645
Chetracin B (NPC470488)		0.7877
Oxyprotostemonine (NPC173173)		0.7644
Stemocurtisine (NPC43648)		0.7569

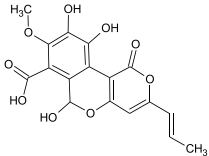
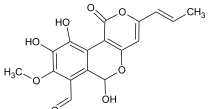
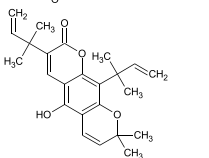
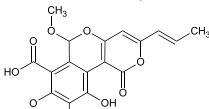
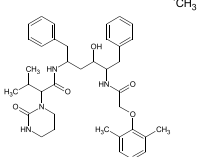
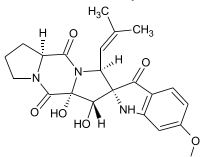
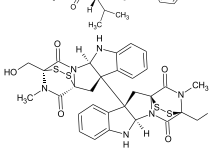
(continued on next page)

Table 1 (continued)

Synthetic drug and the identified NPs	Molecular structure	Similarity score
Munroniamide (NPC176245)		0.7705
Alstobine A (NPC277350)		0.7598
Discorhabdin H (NPC477417)		0.7665
Arbidol		
Phellibaumin A (NPC29411)		0.6838
Difloxacin (NPC318183)		0.7363
Lamellarin D (NPC129897)		0.7175
Lamellarin Gamma Acetate (NPC476995)		0.6682
Hydroxy-6-Methylpyran-2-One Derivative (NPC470989)		0.6822

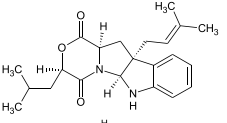
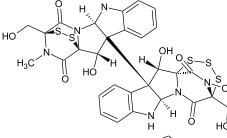
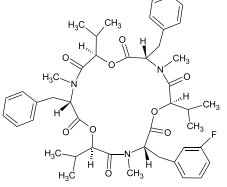
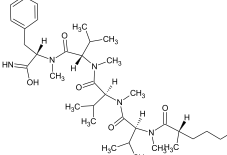
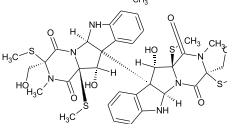
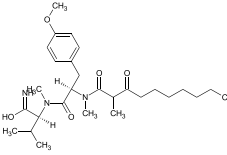
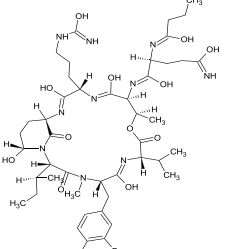
(continued on next page)

Table 1 (continued)

Synthetic drug and the identified NPs	Molecular structure	Similarity score
Cyathuscavin C (NPC474779)		0.7363
Cyathusal B (NPC317781)		0.7135
Clausarin (NPC83535)		0.6770
Cyathuscavin B (NPC474763)		0.7135
Pulvinatal (NPC327652)		0.7010
Lopinavir		
Hexahydrodipyrrolo trione derivative (NPC122886)		0.7458
Beauvericin (NPC89923)		0.7478
Chaetocin (NPC128582)		0.7615

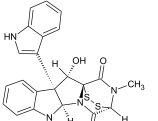
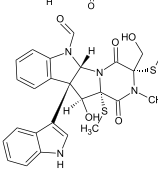
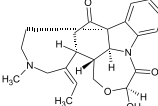
(continued on next page)

Table 1 (continued)

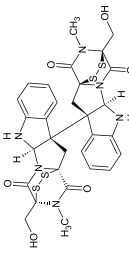
Synthetic drug and the identified NPs	Molecular structure	Similarity score
Mollenine A (NPC285622)		0.7462
Chetracin B (NPC470488)		0.7877
Beauvericin H1 (NPC157311)		0.7549
Dragonamide A (NPC222466)		0.7703
Chetracin D (NPC470491)		0.7892
Dimethyl-3-Oxodecanamide derivative (NPC324081)		0.7569
Symplocamide A (NPC473450)		0.7481
Ritonavir		

(continued on next page)

Table 1 (continued)

Synthetic drug and the identified NPs	Molecular structure	Similarity score
Bionectin B (NPC475859)		0.7146
Luteoalbusin A (NPC470731)		0.6906
Bionectin A (NPC165743)		0.7122
Odioperazine A (NPC297642)		0.7153
Holstiine (NPC11149)		0.6876
Chetracin B (NPC470488)		0.7142
Mollenine A (NPC285622)		0.6796
Methaniminium derivative (NPC194699)		0.7274
Verticillin E (NPC191817)		0.7181

(continued on next page)

Table 1 (continued)	Synthetic drug and the identified NPs	Molecular structure	Similarity score
	Chaetocin (NPC128582)		0.6888

elated natural products were docked against anti-retroviral protease inhibitor (PDB ID 5T6S). During molecular docking, the energy range was set to 3, exhaustiveness to 8, and the number of modes to 9. For the ligand molecules, all the torsions were allowed to rotate during docking. The *in-silico* studies were performed on a local machine equipped with AMD Ryzen 5 six-core 3.4 GHz processor, 8 GB graphics, and 16 GB RAM with Microsoft Windows 10 and Ubuntu 16.04 LTS dual boot operating systems.

2.5. Molecular dynamic simulations to predict the protein structural stability

The structural stability of the free and bound targets was assessed using MD simulations run for a time scale of 20 ns [43,44] by employing the GROMOS96 54a7 [45] force field implemented in the GROMACS-2018 package [46]. A periodic cubic solvated box was created around the target proteins with at least 10 Å distance from the edge of the box and solvated using the simple point charge (SPC) model [47] and neutralized using sodium or chloride ions. The energy minimization was done using the steepest descent method. The system was equilibrated with a temperature coupling at 300K using V-rescale thermostat [48] in NVT ensemble and pressure coupling at 10⁵ Pa using Parrinello-Rahman barostat [49] in NPT ensemble for a period of 500 ps. Bond parameters were adjusted using the LINCS algorithm [50], and the particle mesh Ewald method (PME) [51] was used to evaluate electrostatic interactions. A cut-off at 1.0 nm was set for the long-distance interactions as MD simulation accurately predicts properties of the system for a larger cut-off distance [52]. The final MD trajectories were prepared for a time scale of 20ns at a time step of 2fs with trajectory coordinates updated at 10ps intervals. The final trajectories were analyzed using *gmx energy*, *gmx rms*, *gmx rmsf*, *gmx gyrate*, *gmx do_dssp*, and *gmx sasa* modules of GROMACS along with interaction energies in terms of electrostatic and van der Waals energy between the ligand and the macromolecule.

2.6. Binding free energy calculations using g_mmpbsa

For Molecular mechanics/Poisson-Boltzmann surface area (MMPBSA) calculations, trajectory files were created from the final production MD trajectory with coordinates updated every 200ps. The *g_mmpbsa* package was used for binding energy calculations [53]. The *g_mmpbsa* package uses the following equation to calculate the binding energy of the protein-ligand complex;

$$\Delta G_{\text{Binding}} = G_{\text{Complex}} - (G_{\text{Protein}} + G_{\text{Ligand}}) \quad (I)$$

The 'G' term can be further decomposed into the following components

$$\Delta G = \Delta E_{\text{MM}} + \Delta G_{\text{Solvation}} - T\Delta S = \Delta E_{\text{(Bonded+Non-bonded)}} + \Delta G_{\text{(Polar+Non-polar)}} - T\Delta S \quad (II)$$

Where,

G_{Complex} = total free energy of the binding complex,

G_{Protein} and G_{Ligand} = total free energies of protein and ligand, respectively.

E_{MM} = vacuum potential energy; $G_{\text{Solvation}}$ = free energy of solvation

3. Results

3.1. Structure-based screening of natural products

The natural product library consisting of 26,311 structures was screened against the local Pubchem COVID-19 library of COVID-19 prescribed drugs and COVID-19 clinical trials drug library. Among the total number of molecules screened, 17,798 natural product structures

Table 2A

) Molecular properties and Pharmacokinetics prediction of natural products filtered in for screening against COVID-19 condition.

Identified NPs	Bioavailability and Druglikeness							<i>In silico</i> Pharmacokinetics				
	cLogP	Mol. wt	H-Acceptors	H-Donors	Rotatable Bonds	Total Surface Area	Polar Surface Area	Druglikeness	Human intestinal absorption	Caco-2 permeability	Blood-brain barrier	CYP2D6 substrate
12,28-Oxa-8-Hydroxy-Manzamine A	5.2547	562.755	6	2	1	414.34	60.33	-2.227	0.696+	0.541-	0.800+	0.671-
Alstolobine A	2.4707	398.457	7	1	6	297.41	80.86	-8.1671	0.988+	0.566-	0.896+	0.816-
Beauvericin	5.2239	783.96	12	0	9	610.8	139.83	4.3764	0.991+	0.661+	0.678+	0.825-
Beauvericin H1	5.3247	801.95	12	0	9	617.15	139.83	3.0364	0.990+	0.599+	0.786+	0.829-
Bionectin A	2.9631	450.542	7	3	1	282.66	139.27	5.5488	0.889+	0.508+	0.608+	0.831-
Bionectin B	2.6488	494.595	8	4	2	311.68	159.5	5.0182	0.900-	0.525-	0.832-	0.838-
Bis(Gorgiacerol)Amine	5.4399	757.83	13	3	10	560.06	183.97	-19.005	0.965-	0.616-	0.932-	0.848-
Chaetocin	2.7962	696.852	12	4	3	409.82	246.96	5.8356	0.900+	0.626-	0.661-	0.801-
Chetracin B	1.092	760.916	14	6	3	437.49	312.72	5.4873	0.885+	0.574-	0.816-	0.805-
Chetracin D	0.3976	788.99	14	6	7	496.04	287.42	5.6124	0.922+	0.589-	0.869-	0.805-
Clausarin	5.9768	380.482	4	1	4	295.44	55.76	-5.9217	0.975+	0.840-	0.825+	0.867-
Cyathusal B	0.5256	346.29	8	3	3	243.75	122.52	-4.326	0.915+	0.592+	0.767-	0.909-
Cyathuscavin B	0.5053	376.316	9	3	4	264.22	131.75	-4.7328	0.878+	0.627+	0.775-	0.894-
Cyathuscavin C	0.0774	362.289	9	4	3	248.31	142.75	-2.2479	0.868+	0.592+	0.767-	0.909-
Difloxacin	1.251	399.396	6	1	3	283.48	64.09	5.1997	0.985+	0.879+	0.968-	0.911-
Discorhabdin H	-10.123	762.664	10	3	5	337.61	198.19	2.7192	0.734+	0.603-	0.903-	0.795-
Dragonamide A	3.7111	653.905	10	2	18	539.59	125.32	-3.0172	0.969+	0.543-	0.628-	0.783-
Hexahydrodipyrrolo-trione derivative	0.2123	427.456	9	3	2	288.36	119.41	6.7335	0.946+	0.615-	0.978-	0.802-
Holstiine	1.5964	382.458	6	1	0	270.15	70.08	5.6428	0.972+	0.631+	0.567+	0.784-
Hydroxy-6-Methylpyran-2-One Derivative	5.228	500.586	8	4	11	387.58	141.36	-13.889	0.984+	0.563+	0.660-	0.866-
Lamellarin D	4.3105	499.474	9	3	4	352.71	119.09	1.8379	0.983+	0.604+	0.606+	0.448-
Lamellarin Gamma Acetate	5.3	573.596	10	1	8	423.68	106.84	2.3739	0.987+	0.683+	0.747+	0.628-
Luteoalbusin A	3.1416	464.569	7	3	2	295.59	139.27	5.9847	0.890+	0.581-	0.575+	0.812-
Marineosin A	4.6896	409.572	5	2	2	323.4	62.4	-2.232	0.986+	0.638-	0.824+	0.764-
Methaniminium derivative	-0.4649	910.463	21	10	14	679.31	329.1	6.1103	0.795+	0.647-	0.976-	0.831-
Methylstemofoline	0.9975	345.394	6	0	1	220.03	57.23	4.0559	0.922+	0.670+	0.679+	0.741-
Mollenine A	3.3511	368.475	5	1	4	275.46	58.64	3.6919	0.980+	0.516-	0.608+	0.824-
Munroniamide	-0.4894	597.663	12	2	7	419.88	166.86	-8.9989	0.940+	0.628-	0.500+	0.808-
Odioperazine A	1.9865	538.647	9	3	4	357.08	167.78	6.2082	0.843+	0.510-	0.807-	0.506-
Oxyprotostemonine	1.004	431.483	8	0	2	289.89	83.53	2.3627	0.890+	0.648+	0.549+	0.803-
Phellibaumin A	2.8483	352.297	7	4	2	248.17	120.36	0.0022	0.952+	0.828-	0.725+	0.905-
Pulvinatal	0.9535	360.317	8	2	4	259.66	111.52	-6.9354	0.919+	0.627+	0.775-	0.894-
Stemocurtisine	1.4247	347.41	6	0	1	239.64	57.23	2.9196	0.922+	0.668+	0.758+	0.744-
Symplocamide A	0.6976	1052.03	23	11	18	763.41	359.52	1.3524	0.915+	0.634-	0.959-	0.830-
Verticillin E	1.7482	752.872	14	4	3	439.8	281.1	4.5639	0.895+	0.536-	0.836-	0.825-

were found to have more than 60% structural similarities against the Pubchem COVID-19 library entries, of which 41 molecules were flavans, 41 were flavones, and 272 were isoflavonoids. The comparison against clinical trials drug library yielded 14,689 natural products with more than 60% structure similarity consisting of 30 flavans, 18 flavones, and 78 isoflavonoids. The study was extended to compare the complete natural product library against the most promising investigational drugs, viz. Remdesivir, Arbidol, Lopinavir, and Ritonavir molecules. This comparison yielded a total of 35 natural product structures with more than 60% structural similarity. The natural products with structural similarities to respective investigational drugs are detailed in Table 1.

3.2. Molecular properties based PK/PD analysis

Molecular properties and Pharmacokinetics prediction of natural products were predicted using Osiris data warrior software and the

admetSAR server. The drug-likeness estimated based on the molecular properties of the selected structures indicated that out of 35 molecules, 23 molecules with positive scores indicated their potential drug-like effects (Table 2A). Gastrointestinal (GI) absorption is an important parameter to screen orally administered drugs. A positive value shown in Table 2A for gastrointestinal (GI) absorption suggests a high probability of success for absorption into the intestinal tract [54]. While the blood-brain barrier (BBB) penetration indicates the potential of a drug to cross into the brain, it can bind to specific receptors and activate specific signaling pathways. Therefore, the prediction of BBB penetration is crucial in the drug development pipeline [55]. In the present study, 33 molecules were found to penetrate the human intestine barrier, 17 molecules penetrating the blood-brain barrier. None of them was the substrate for Cytochromes P450 group of isozymes that regulates drug metabolism, indicating a high possibility of their bioavailability (Table 2A). Further, out of 35 molecules, 34 were predicted to be non-mutagenic, non-tumorigenic, and non-irritant, with 10 molecules

Table 2B) *In-silico* Pharmacodynamics prediction of natural products selected for screening against COVID-19 condition.

Identified NPs	Mutagenic	Tumorigenic	Reproductive effective	Ocular irritancy	Aerobic biodegradability	Ames toxicity score	Carcinogen
12,28-Oxa-8-Hydroxy-Manzamine A	NONE	NONE	NONE	0.946-	1.00-	0.707-	0.607-
Alstolobine A	NONE	HIGH	NONE	0.979-	1.00-	0.714-	0.573-
Beauvericin	NONE	NONE	NONE	0.925-	0.912-	0.772-	0.622-
Beauvericin H1	NONE	NONE	NONE	0.922-	0.996-	0.776-	0.536-
Bionectin A	NONE	NONE	NONE	0.972-	0.986-	0.733-	0.609-
Bionectin B	NONE	NONE	NONE	0.965-	0.988-	0.870-	0.611-
Bis(Gorgiacerol)Amine	NONE	NONE	HIGH	0.901-	0.623-	0.573-	0.487-
Chaetocin	NONE	NONE	NONE	0.918-	0.994-	0.645-	0.623-
Chetracin B	NONE	NONE	NONE	0.911-	0.973-	0.679-	0.644-
Chetracin D	NONE	NONE	NONE	0.904-	0.996-	0.678-	0.627-
Clausarin	NONE	NONE	HIGH	0.607+	0.993-	0.506-	0.472-
Cyathusal B	NONE	NONE	HIGH	0.561-	0.937-	0.707+	0.465-
Cyathuscavin B	NONE	NONE	HIGH	0.590-	0.966-	0.712+	0.515+
Cyathuscavin C	NONE	NONE	HIGH	0.574-	0.937-	0.707+	0.465-
Difloxacin	NONE	NONE	NONE	0.949-	1.00-	0.885+	0.610-
Discorhabdin H	NONE	NONE	NONE	0.960-	1.00-	0.593-	0.532-
Dragonamide A	NONE	NONE	NONE	0.922-	1.00-	0.812-	0.678-
Hexahydrodipyrrolo trione derivative	NONE	NONE	NONE	0.927-	1.00-	0.658-	0.597-
Holstiine	NONE	NONE	NONE	0.986-	0.951-	0.572-	0.501-
Hydroxy-6-Methylpyran-2-One Derivative	NONE	NONE	NONE	0.732-	0.500+	0.815-	0.723-
Lamellarin D	NONE	NONE	HIGH	0.833-	0.993-	0.586-	0.389-
Lamellarin Gamma Acetate	NONE	NONE	HIGH	0.989-	0.995-	0.880-	0.599-
Luteoalbusin A	NONE	NONE	NONE	0.986-	0.987-	0.670-	0.630-
Marineosin A	NONE	NONE	NONE	0.972-	1.00-	0.655-	0.651-
Methaniminium derivative	NONE	NONE	NONE	0.905-	0.962-	0.615-	0.570-
Methylstemofoline	NONE	NONE	NONE	0.891-	1.00-	0.755-	0.470-
Mollenine A	NONE	NONE	NONE	0.986-	0.997-	0.572-	0.528-
Munroniamide	LOW	HIGH	LOW	0.978-	1.00-	0.512-	0.562-
Odioperazine A	NONE	NONE	NONE	0.987-	0.997-	0.670-	0.606-
Oxyprotostemonine	NONE	NONE	NONE	0.943-	0.994-	0.681-	0.440-
Phellibaumin A	HIGH	NONE	HIGH	0.528-	0.911-	0.550+	0.419-
Pulvinatal	NONE	NONE	HIGH	0.547-	0.966-	0.712+	0.515+
Stemocurtisine	NONE	NONE	NONE	0.914-	0.995-	0.781-	0.420-
Symplocamide A	NONE	NONE	NONE	0.901-	0.945-	0.644-	0.594-
Verticillin E	NONE	NONE	HIGH	0.900-	0.986-	0.763-	0.610-

predicted to have reproductive effects (Table 2B). Among the 35 structures, 29 compounds were non-AMES toxic, 34 non-carcinogens, and 34 were not readily biodegradable.

3.3. Molecular interactions studies using automated docking

The *in-silico* molecular interaction studies were used to predict the most effective natural product drug to bind to the appropriate target involved in the regulation of virus entry, replication, assembly, and release, as well as host-specific interactions. In the present study, the docking studies were carried out for synthetic antiviral agents as well as their structurally similar natural products against different targets proteins of SARS-CoV-2 to deduce the structural insight of molecular interactions. The study yielded natural products being effectively bound to their respective targets (Table 3). The results were expressed in terms of docking energy (kcal/mol). Many selected natural products have displayed docking energies lower than their structurally similar standard drug counterparts. The natural products similar to Remdesivir interact with SARS-CoV NSP12 polymerase with docking energies comparably lower than the standard drug. The natural products tested as influenza virus hemagglutinin inhibitors are also bound to the target with docking energies lower than the standard drug arbidol. The binding interactions of natural products tested as viral protease inhibitors were compared with standard drugs Lopinavir and Ritonavir. The effectiveness of these

binding of natural products with the highest interaction energy in each group was selected for protein stability assessment using molecular dynamics simulations (Fig. 4).

3.4. Molecular dynamic simulations to predict the protein structural stability

In the present study, united-atom MD simulations were performed to confirm the accuracy of binding resulting from docking studies [56]. The result of the MD simulation displayed the conformational changes acquired by different target proteins of SARS-CoV-2 upon binding and inferred the structural insight on molecular stability (Fig. 5).

The RMSD analysis was done to understand the deviation of C α atoms of the protein from its backbone, and RMSF analysis was done to study the fluctuations associated with the amino acid residues of the protein during the simulation. The average RMS deviations and RMS fluctuations were calculated from the MD trajectories of natural product, and synthetic drug bound HIV-1 protease (I50V isolate), Influenza virus hemagglutinin, SARS-CoV NSP 12 polymerase, and HIV-1 protease (A02 isolate) and were compared with their respective unbound structures (Table 4). The RMSD plots indicate that Remdesivir bound SARS CoV NSP 12 polymerase (Fig. 4a) and Arbidol bound Influenza virus hemagglutinin (Fig. 4b) displayed lesser deviations than their structurally similar natural products, Hydroxy Manzamin A and Phellibaumin_A

Table 3

Molecular interactions between the selected natural products with targets of their structurally similar chemical drugs expressed as docking energies along with their structure similarity score. The table also details the number of hydrogen bonds formed between the Natural product and the amino acid residues from the target molecule.

Target protein	Synthetic drug and the identified NPs	Docking Energy ^a	H-bonds	Receptor residues involved in H-bond formation	
SARS-CoV NSP12 POLYMERASE	Remdesivir	-7.2	03	ILE23, LEU126, GLY48	
	12,28-Oxa-8-Hydroxy-Manzamine A	-10.4	02	GLY130, ALA38	
	Marineosin A	-7.9	00	-	
	Bis(Gorgiacerol)Amine	-7.8	02	ILE23, GLY130	
	Methylstemofoline	-7.7	02	SER128, ALA129	
	Chetracin B	-7.5	01	PHE156	
	Oxyprotostemonine	-7.5	02	SER128, ALA129	
	Stemocurtisine	-7.5	01	GLY48	
	Munroniamide	-6.9	05	VAL49, ILE131, GLY48, GLY130, LEU126	
	Alstoboline A	-6.8	03	PHE156, ASP157, ALA154	
	Discorhabdin H	-6.7	02	GLY48, ASP22	
	INFLUENZA VIRUS HEMAGGLUTININ	Arbidol	-7.1	01	GLU64
		Phellibaumin A	-9.4	04	ASP280, SER290, LYS58, ILE288
Difloxacin		-8.4	03	LYS58, LEU292, PRO293	
Lamellarin D		-8.4	02	LYS58, CYS305	
Lamellarin Gamma Acetate		-7.8	01	GLU57	
Hydroxy-6-Methylpyran-2-One Derivative		-7.6	03	THR59, GLU57, THR59	
Cyathuscavin C		-7.5	02	GLU57, PRO306	
Cyathusal B		-7.4	02	GLU57, PRO306	
Clausarin		-7.3	02	GLU64, ARG85	
Cyathuscavin B		-7.3	00	-	
Pulvinatal		-7.3	01	THR59	
HIV-1 PROTEASE I50V ISOLATE		Lopinavir	-6.5	03	GLY49, GLY51, GLY52
		Hexahydrodipyrrolo trione derivative	-8.4	03	PRO81, ASP25, GLY48
	Beauvericin	-7.2	01	GLY49	
	Chaetocin	-7.1	06	THR74, ASN88, GLN92, ASP30, ILE72, GLY73	
	Mollenine A	-7.1	00	-	
	Chetracin B	-6.9	00	-	
	Beauvericin H1	-6.6	00	VAL50, GLY51, THR80	
	Dragonamide A	-6.3	02	ASP30, VAL50	
	Chetracin D	-6.2	04	THR74, ARG87, ASP29, GLY73	
	Dimethyl-3-Oxodecanamide derivative	-5.6	03	VAL50, GLY51, PHE53	
	Symplocamide A	-4.6	00	-	
	HIV-1 PROTEASE A02 ISOLATE	Ritonavir	-7.7	04	ASP29, ASP30, GLY48, GLY49
		Bionectin B	-8.1	03	ILE50, THR82, GLY51
Luteoalbusin A		-8.0	04	GLY51, GLY52, PRO81, PRO79	
Bionectin A		-7.7	02	THR96, ASN98	
Odioperazine A		-7.7	02	ILE50, ASP25	
Holstiine		-7.1	00	-	
Chetracin B		-7.0	02	ARG87, LUE97	
Mollenine A		-6.9	00	-	
Methaniminium derivative		-6.6	01	PRO81	
Verticillin E		-6.6	02	THR74, ASN88	
Chaetocin		-6.4	02	ARG08, THR26	

^a kcal/mol.

bound structures. However, the macromolecular structures HIV-1 protease (I50V isolate) (Fig. 4c) and HIV-1 protease (A02 isolate) (Fig. 4d) displayed lesser RMS deviations upon binding with respective natural products compared to their synthetic drug counterparts. It can also be seen from these plots that the deviations in the macromolecular structures are relatively low after 5ns in both conditions. From the RMSF plots (Fig. 4e-h), it can be inferred that, though the residues displayed minor fluctuations at certain positions, all proteins were able to retain their secondary structure's packability. This was inferred based on the Rg plots (Fig. 5i-l), where the structures were found to be very tightly packed, as the secondary structure elements like α -helix, β -sheet, and turn were remodeled at each time step of the MD simulation. The SASA plots (Fig. 5m-p) also supported these findings.

The binding free energy calculations performed using the g_mmpba module displayed better binding of natural products with their respective target proteins. The binding free energies of natural products,

12,28-Oxa-8-Hydroxy-Manzamine A (-57.17 kJ/mol), Phellibaumin A (-60.86 kJ/mol), and Bionectin B (-161.08 kJ/mol) were found to be encouraging in deducing their interactions with their respective targets. However, their structurally similar synthetic drug counterparts viz. Remdesivir (-63.68 kJ/mol), Arbidol (-104.39 kJ/mol), and Ritonavir (-180.45 kJ/mol) displayed higher binding free energies towards their respective targets. Nevertheless, the binding free energy of the natural product Hexahydrodipyrrolo trione derivative (-93.53 kJ/mol) was found to be higher than its structurally similar standard drug counterparts; Lopinavir (-77.59 kJ/mol). The associated terms for binding free energy calculations along with the calculated MD parameters for unbound and ligand-bound targets detailing RMSD, RMSF, Rg, SASA, Secondary structure, Coul-SR energy, and LJ-SR energy are detailed in Table 4.

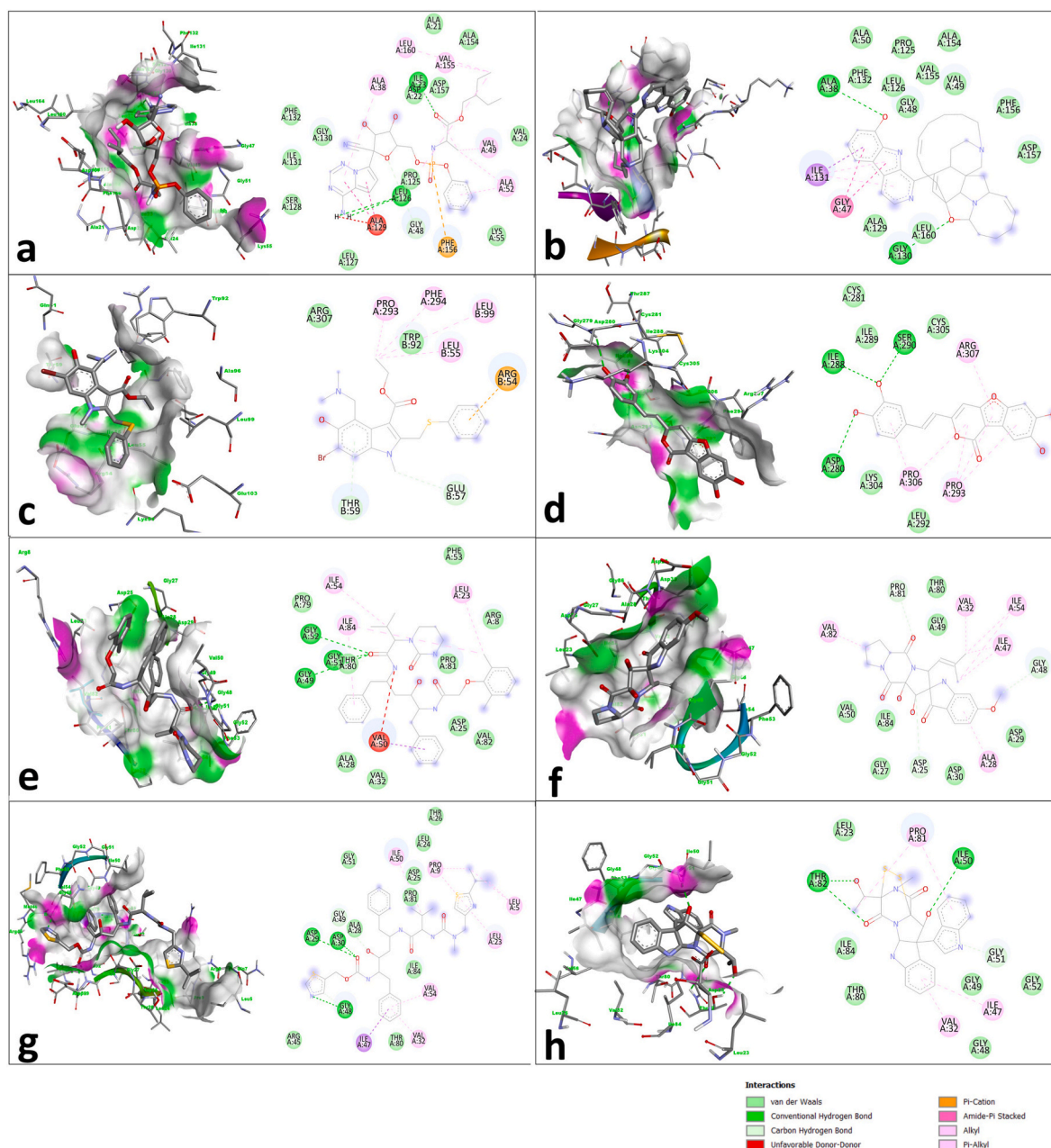


Fig. 4. Docking interaction between Remdesivir (a), and 12,28-Oxa-8-Hydroxy-Manzamine A (b) with SARS-CoV NSP12 polymerase, Arbidol (c), and Phellibaumin A (d) with influenza virus hemagglutinin, Lopinavir (e), and Hexahydrodipyrrolo trione derivative (f) with HIV-1 protease I50V isolate and Ritonavir (g), and Bionectin B (h) with HIV-1 protease A02 isolate.

4. Discussion

Viral infections have always created challenges in human healthcare research. Identifying efficacious and cost-effective antiviral drugs in the absence of potential vaccines or standard therapies thus holds utmost importance. Due to the advancements in virology, molecular biology, and computational biology, we can now decipher the pathophysiology of many viral diseases, including COVID-19 infection [57]. Natural products have been playing an important role as complementary medicine to combat viral infections, and herbal medicines have been an

excellent source for modern drug research programs for a long time [58]. Their origin, availability, safety, and cost-effectiveness make them a reliable choice alongside modern medicine [59].

With the advancements in computational techniques, new strategies have been designed to predict the interactions of potential human target proteins with specific viral strains [60]. These models rely on the available interaction information to predict the novel host-virus interactions. These predictions have been reliable in the past in understanding the infection mechanism of SARS-CoV [61], MERS-CoV [61], Ebola virus [62], and Zika virus [63]. However, these computational

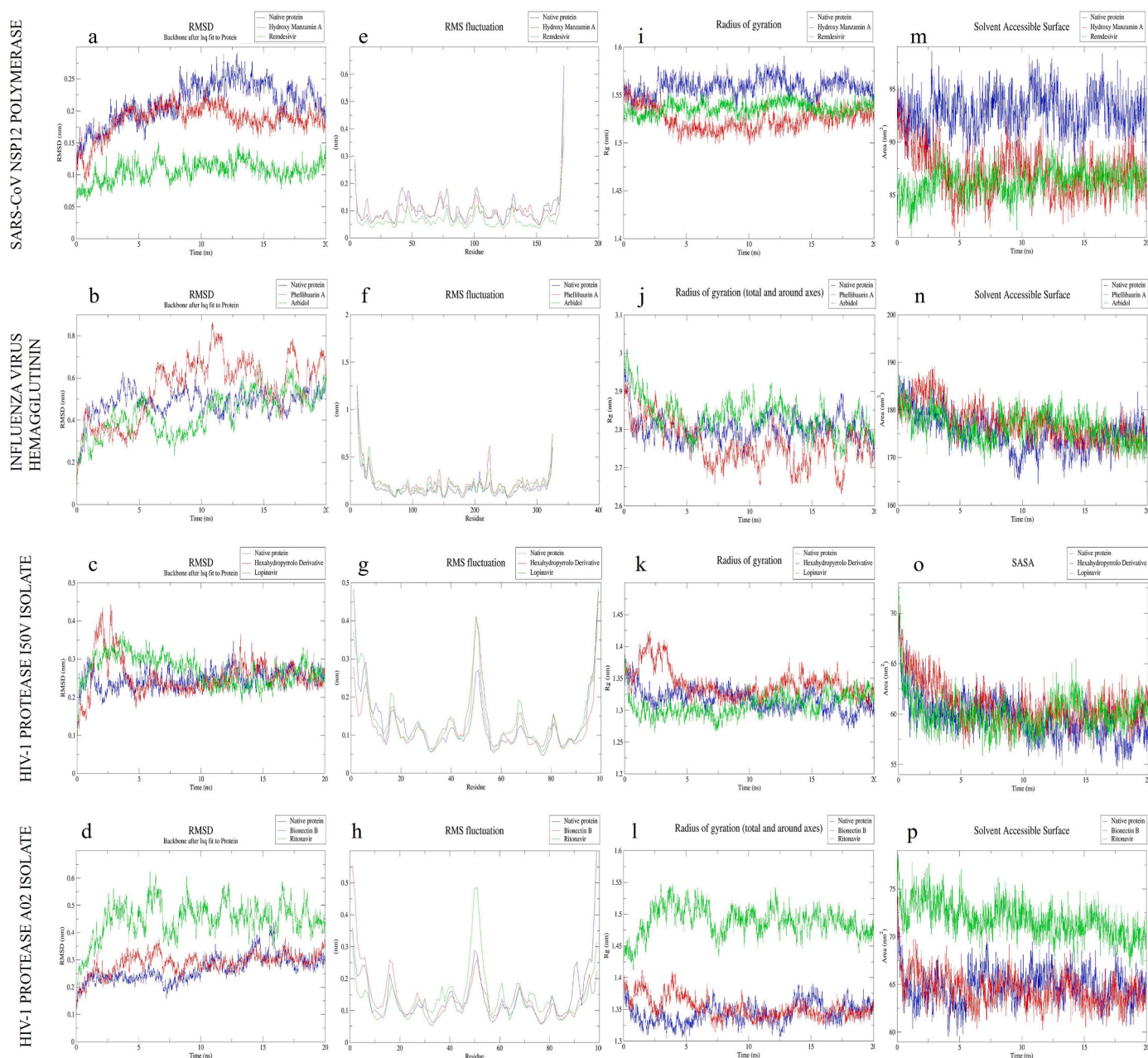


Fig. 5. RMSD (a–d), RMSF (e–h), Rg (i–l) and SASA (m–p) plots obtained from MD trajectories analysis of native, Natural product bound, and chemical drug bound structure of SARS-CoV NSP12 polymerase, influenza virus hemagglutinin, and HIV-1 protease of I50V isolate and A02 isolate.

methods play a significant role in modern drug research; the experimental verifications of virus-host interactions are needed to substantiate the potential interactions [64–66]. Along with this, the availability of verified interactions and relevant information is a prerequisite for computational drug discovery methods. Most of the chemical structure search and identification methods today rely on the conventional string search to modern data structure module-based approaches [67–70]. The structural comparison and screening based on physicochemical properties, topological indices, molecular graphs, pharmacophore features, molecular shapes, molecular fields, and quantitative measures are

expected to reduce false-positive results and yield more effective structures [13,14]. In the current investigation, we were able to shortlist some of the natural products as potential drug-like molecules based on their structural similarities with synthetic chemical drugs. The screening is based on the central foundation of medicinal chemistry that the structurally similar molecules will have similar biological effects [12, 14]. The yielded structures were docked to the binding site of the target protein of their respective structurally similar synthetic drugs. To confirm the structural stability, molecular dynamic simulation studies were performed, and the results were compared with unbound and

Table 4
Calculated MD parameters for native and ligand-bound SARS CoV2 drug targets obtained from the MD simulation along with binding energies and the contributing energy terms of the prescribed drugs and their most similar natural product calculated using g.mmpbsa module.

Gromacs Modules	SARS-CoV NSP12 POLYMERASE			INFLUENZA VIRUS HEMAGGLUTININ			HIV-1 PROTEASE I50V ISOLATE			HIV-1 PROTEASE A02 ISOLATE		
	Native Protein	Remdesivir	12,28-Oxa-8-Hydroxy-Manzamine A	Native Protein	Arbidol	Phellibaumin A	Native Protein	Lopinavir	Hexahydrodipyrrolo trione derivative	Native Protein	Ritonavir	Bionectin B
Potential Energy (x 10 ⁻⁶)	-0.638	-0.638	-0.637	-4.605	-4.604	-4.604	-0.436	-0.434	-0.436	-0.519	-0.518	-0.518
RMSD (nm)	0.213	0.195	0.186	0.481	0.429	0.549	0.247	0.270	0.254	0.265	0.447	0.287
RMSF (nm)	0.105	0.055	0.099	0.176	0.216	0.231	0.130	0.141	0.130	0.140	0.144	0.139
Rg (nm)	1.558	1.523	1.524	2.802	2.835	2.763	1.316	1.307	1.342	1.343	1.488	1.352
SASA (nm ²)	92.95	85.00	87.13	175.24	176.47	177.43	59.57	60.05	60.92	64.83	71.84	64.44
Secondary Structure	210.49	221.97	219.29	283.92	295.63	285.29	119.47	112.07	118.78	117.81	117.54	120.51
Coul-SR ^a	-	-47.22	-3.84	-	-9.45	-65.80	-	-40.29	-30.24	-	-83.47	-66.90
LJ-SR ^a	-	-92.72	-64.15	-	-109.61	-114.98	-	-113.62	-109.54	-	-326.78	-160.13
Binding Energy ^a	-	-63.68	-57.17	-	-104.39	-60.86	-	-77.59	-93.53	-	-180.45	-161.08
SASA Energy ^a	-	-19.36	-8.68	-	-14.03	-13.62	-	-14.11	-13.84	-	-34.91	-16.52
Polar Solvation Energy ^a	-	146.39	35.27	-	43.27	132.86	-	97.20	67.11	-	179.49	73.50
Electrostatic Energy ^a	-	-36.09	-3.27	-	-6.71	-51.28	-	-29.45	-17.77	-	-49.11	-32.73
van der Waals Energy ^a	-	-154.62	-80.48	-	-126.92	-128.81	-	-131.22	-129.03	-	-375.91	-185.33

^a kcal/mol.

synthetic drug-bound macromolecular structures. The results identified the selected natural products as potential drug leads, and with critical screening, could serve as promising molecules in the first-line treatment for COVID-19 infections. Several studies have also shown the therapeutic potentials of natural products and their interactions with the key viral proteins associated with virulence [9,71–74]. Nevertheless, the future studies comprising *in-vitro* studies targeting specific proteins followed by their *in-silico* structure stability assessment with nano and microsecond simulations will validate their use as potential therapeutic molecules.

Ethics approval and consent to participate

Not applicable.

Funding

This work is an extension of a research project supported by the Department of Science and Technology (DST)- Science and Engineering Research Board (SERB), Govt. of India (Grant number: PDF/2018/00237).

Consent for publication

Not applicable.

Availability of data and materials

All the data used during the current study are available from the corresponding author on reasonable request.

CRedit authorship contribution statement

S.J. Aditya Rao: Conceptualization, Investigation, Methodology, Software, Validation, Writing – original draft, Writing – review & editing. **Nandini P. Shetty:** Formal analysis, Supervision, Writing – review & editing.

Declaration of competing interest

The authors declare that, the above mentioned manuscript has not been published and is not under consideration for publication elsewhere. The authors are aware of the submission and have no conflicts of interest to disclose.

Data availability

Data will be made available on request.

Acknowledgment

The authors thank the Department of Science and Technology (DST) - Science and Engineering Research Board (SERB), Govt. of India for their financial support.

Abbreviations

ADME	Absorption, Distribution, Metabolism, and Excretion
APBS	Adaptive Poisson-Boltzmann Solver
HTVS	High Throughput Virtual Screening
MD	Molecular Dynamics
MM	Molecular mechanical
MMPBSA	Molecular mechanics/Poisson-Boltzmann surface area
NCATS	National Center for Advancing Translational Sciences
NPASS	Natural product activity and species source database
NPs	Natural products

PD	Pharmacodynamics
PDB	Protein Data Bank
PK	Pharmacokinetics
PME	Particle Mesh Ewald method
Rg	Radius of Gyration
RMSD	Root Mean Square Deviation
RMSF	Root Mean Square Fluctuation
RO5	Rule-of-Five
SASA	Solvent Accessible Surface Area
SMILES	Simplified Molecular Input Line Entry System
SPC	Simple Point Charge
TPSA	Topological polar surface area

Appendix A. Supplementary data

Supplementary data to this article can be found online at <https://doi.org/10.1016/j.micpath.2022.105497>.

References

- [1] L.T. Lin, W.C. Hsu, C.C. Lin, Antiviral natural products and herbal medicines, *J. Tradit. Complement. Med.* 4 (2014) 24–35, <https://doi.org/10.4103/2225-4110.124335>.
- [2] X. Li, W. Wang, X. Zhao, J. Zai, Q. Zhao, Y. Li, A. Chaillon, Transmission dynamics and evolutionary history of 2019-nCoV, *J. Med. Virol.* 92 (2020) 501–511, <https://doi.org/10.1002/jmv.25701>.
- [3] WHO, Global research on coronavirus disease (COVID-19). <https://www.who.int/emergencies/diseases/novel-coronavirus-2019/global-research-on-novel-coronavirus-2019-ncov>, 2021.
- [4] S.U. Rehman, L. Shafique, A. Ihsan, Q. Liu, Evolutionary trajectory for the emergence of novel coronavirus SARS-CoV-2, *Pathogens* 9 (2020), <https://doi.org/10.3390/pathogens9030240>.
- [5] J. Harcourt, A. Tamin, X. Lu, S. Kamili, S.K. Sakthivel, J. Murray, K. Queen, Y. Tao, C.R. Paden, J. Zhang, Y. Li, A. Uehara, H. Wang, C. Goldsmith, H.A. Bullock, L. Wang, B. Whitaker, B. Lynch, R. Gautam, C. Schindewolf, K.G. Lokugamage, D. Scharton, J.A. Plante, D. Mirchandani, S.G. Widen, K. Narayanan, S. Makino, T. G. Ksiazek, K.S. Plante, S.C. Weaver, S. Lindstrom, S. Tong, V.D. Menachery, N. J. Thornburg, Severe acute respiratory syndrome coronavirus 2 from patient with coronavirus disease, United States, *Emerg. Inf. Disp.* 26 (2020) 1266–1273, <https://doi.org/10.3201/EID2606.200516>.
- [6] W. Wang, J. Tang, F. Wei, Updated understanding of the outbreak of 2019 novel coronavirus (2019-nCoV) in Wuhan, China, *J. Med. Virol.* 92 (2020) 441–447, <https://doi.org/10.1002/jmv.25689>.
- [7] J.F.W. Chan, S. Yuan, K.H. Kok, K.K.W. To, H. Chu, J. Yang, F. Xing, J. Liu, C.C. Y. Yip, R.W.S. Poon, H.W. Tsoi, S.K.F. Lo, K.H. Chan, V.K.M. Poon, W.M. Chan, J. D. Ip, J.P. Cai, V.C.C. Cheng, H. Chen, C.K.M. Hui, K.Y. Yuen, A familial cluster of pneumonia associated with the 2019 novel coronavirus indicating person-to-person transmission: a study of a family cluster, *Lancet* 395 (2020) 514–523, [https://doi.org/10.1016/S0140-6736\(20\)30154-9](https://doi.org/10.1016/S0140-6736(20)30154-9).
- [8] H. Li, Z. Liu, J. Ge, Scientific research progress of COVID-19/SARS-CoV-2 in the first five months, *J. Cell Mol. Med.* 24 (2020) 6558–6570, <https://doi.org/10.1111/jcmm.15364>.
- [9] R. Chilamakuri, S. Agarwal, COVID-19: characteristics and therapeutics, *Cells* 10 (2021), <https://doi.org/10.3390/cells10020206>.
- [10] H. Yuan, Q. Ma, L. Ye, G. Piao, The traditional medicine and modern medicine from natural products, *Molecules* 21 (2016), <https://doi.org/10.3390/molecules21050559>.
- [11] C.T. Walsh, Y. Tang, *Natural Product Biosynthesis*, The Royal Society of Chemistry, 2017.
- [12] Y.C. Martin, J.L. Kofron, L.M. Traphagen, Do structurally similar molecules have similar biological activity? *J. Med. Chem.* 45 (2002) 4350–4358, <https://doi.org/10.1021/jm020155c>.
- [13] D. Gfeller, A. Grosdidier, M. Wirth, A. Daina, O. Michielin, V. Zoete, SwissTargetPrediction: a web server for target prediction of bioactive small molecules, *Nucleic Acids Res* 42 (2014), <https://doi.org/10.1093/nar/gku293>.
- [14] A. Kumar, K.Y.J. Zhang, Advances in the development of shape similarity methods and their application in drug discovery, *Front. Chem.* 6 (2018), <https://doi.org/10.3389/fchem.2018.00315>.
- [15] M.S. Nobile, P. Cazzaniga, A. Tangherloni, D. Besozzi, Graphics processing units in bioinformatics, computational biology and systems biology, *Briefings Bioinf.* 18 (2017) 870–885, <https://doi.org/10.1093/bib/bbw058>.
- [16] S.J. Aditya Rao, C.K. Ramesh, S. Raghavendra, M. Paramesha, Dehydroabietylamine, A diterpene from carthamus tinctorious L. Showing antibacterial and anthelmintic effects with computational evidence, *Curr. Comput. Aided Drug Des.* 16 (2020) 231–237, <https://doi.org/10.2174/1573409915666190301142811>.
- [17] S.J. Gange, E.T. Golub, From smallpox to big data: the next 100 years of epidemiologic methods, *Am. J. Epidemiol.* 183 (2016) 423–426, <https://doi.org/10.1093/aje/kwv150>.
- [18] A.B. Docherty, N.I. Lone, Exploiting big data for critical care research, *Curr. Opin. Crit. Care* 21 (2015) 467–472, <https://doi.org/10.1097/MCC.0000000000000228>.
- [19] C.S. Greene, J. Tan, M. Ung, J.H. Moore, C. Cheng, Big data bioinformatics, *J. Cell. Physiol.* 229 (2014) 1896–1900, <https://doi.org/10.1002/jcp.24662>.
- [20] T. Wasser, K. Haynes, J. Barron, M. Cziraky, Using “big data” to validate claims made in the pharmaceutical approval process, *J. Med. Econ.* 18 (2015) 1013–1019, <https://doi.org/10.3111/13696998.2015.1108919>.
- [21] S. Raghavendra, S.J. Aditya Rao, V. Kumar, C.K. Ramesh, Multiple ligand simultaneous docking (MLSD): a novel approach to study the effect of inhibitors on substrate binding to PPO, *Comput. Biol. Chem.* 59 (2015) 81–86, <https://doi.org/10.1016/j.compbiolchem.2015.09.008>.
- [22] A.R.S. Janakirama, S.M. Shivayogi, J.K. Satyanarayana, R.C. Kumaran, Characterization of isolated compounds from *Morus* spp. and their biological activity as anticancer molecules, *Bioimpacts* 11 (2021) 187–197, <https://doi.org/10.34172/bi.2021.09>.
- [23] P.R. Arantes, A. Saha, G. Palermo, Fighting covid-19 using molecular dynamics simulations, *ACS Cent. Sci.* 6 (2020) 1654–1656, <https://doi.org/10.1021/acscentsci.0c01236>.
- [24] Dr. Duke’s phytochemical and ethnobotanical databases, U S Dep. Agric. Agric. Res. Serv. (REP). 1992-2016. (n.d.). <https://doi.org/10.15482/USDA.ADC/1239279>.
- [25] X. Zeng, P. Zhang, W. He, C. Qin, S. Chen, L. Tao, Y. Wang, Y. Tan, D. Gao, B. Wang, Z. Chen, W. Chen, Y.Y. Jiang, Y.Z. Chen, NPASS: natural product activity and species source database for natural product research, discovery and tool development, *Nucleic Acids Res* 46 (2018) D1217–D1222, <https://doi.org/10.1093/nar/gkx1026>.
- [26] K. Das, S. Gezici, Review article Plant secondary metabolites, their separation, identification and role in human disease prevention, *Ann. Phytomedicine An Int. J.* 7 (2018) 13–24, <https://doi.org/10.21276/ap.2018.7.2.3>.
- [27] R.A. Hussein, A.A. El-Anssary, Plants Secondary Metabolites: the Key Drivers of the Pharmacological Actions of Medicinal Plants, *Herb. Med.*, 2019, <https://doi.org/10.5772/intechopen.76139>.
- [28] B. Singh, T.K. Bhat, B. Singh, Potential therapeutic applications of some antinutritional plant secondary metabolites, *J. Agric. Food Chem.* 51 (2003) 5579–5597, <https://doi.org/10.1021/jf021150r>.
- [29] S. Kim, J. Chen, T. Cheng, A. Gindulyte, J. He, S. He, Q. Li, B.A. Shoemaker, P. A. Thiessen, B. Yu, L. Zaslavsky, J. Zhang, E.E. Bolton, PubChem 2019 update: improved access to chemical data, *Nucleic Acids Res* 47 (2019), D1102–D1109, <https://doi.org/10.1093/nar/gky1033>.
- [30] U.S. National Institute of Health (NIH), U.S. National Library of Medicine (NLM), ClinicalTrials.gov Database, U.S. Natl. Libr. Med., 2008. <https://clinicaltrials.gov/ct2/home>.
- [31] T. Sander, J. Freyss, M. Von Korff, C. Rufener, DataWarrior: an open-source program for chemistry aware data visualization and analysis, *J. Chem. Inf. Model.* 55 (2015) 460–473, <https://doi.org/10.1021/ci500588j>.
- [32] G. Divyashri, T.P.K. Murthy, S. Sundareshan, P. Kamath, M. Murahari, G. R. Saraswathy, B. Sadanandan, In silico approach towards the identification of potential inhibitors from *Curcuma amada* Roxb against *H. pylori*: ADMET screening and molecular docking studies, *Bioimpacts* 11 (2020) 119–127, <https://doi.org/10.34172/BI.2021.19>.
- [33] B. Kikiowo, A.J. Ogunleye, O.K. Inyang, N.S. Adelakun, O.I. Omotuyi, D. S. Metibemu, T.I. David, O.O. Oludoyi, T.T. Ijatuyi, Flavones scaffold of chromolaena odorata as a potential xanthine oxidase inhibitor: induced fit docking and ADME studies, *Bioimpacts* 10 (2020) 227–234, <https://doi.org/10.34172/bi.2020.29>.
- [34] S.J. Aditya Rao, N. Shetty, Structure-based Assessment of Homologous Analogues of Natural products: a computational approach to predict the therapeutic effects of natural products, *Res. Sq.* (2021), <https://doi.org/10.21203/rs.3.rs-620117/v1>.
- [35] J.-H. Liu, B.-Y. Yu, Biotransformation of bioactive natural products for pharmaceutical lead compounds, *Curr. Org. Chem.* 14 (2010) 1400–1406, <https://doi.org/10.2174/138527210791616786>.
- [36] C.A. Lipinski, F. Lombardo, B.W. Dominy, P.J. Feeney, Experimental and computational approaches to estimate solubility and permeability in drug discovery and development settings, *Adv. Drug Deliv. Rev.* 23 (1997) 3–25, [https://doi.org/10.1016/S0169-409X\(96\)00423-1](https://doi.org/10.1016/S0169-409X(96)00423-1).
- [37] B.C. Doak, B. Over, F. Giordanetto, J. Kihlberg, Oral druggable space beyond the rule of 5: insights from drugs and clinical candidates, *Chem. Biol.* 21 (2014) 1115–1142, <https://doi.org/10.1016/j.chembiol.2014.08.013>.
- [38] S.J. Aditya Rao, T. Venugopal, N. Jayanna, M. Paramesha, C. Ramesh, Bioactive isolates of *Morus* species as antibacterial agents and their in silico profiling, *Lett. Drug Des. Discov.* 18 (2021) 445–453, <https://doi.org/10.2174/1570180817999201104120815>.
- [39] A. Jarrahpour, M. Motamedifar, M. Zarei, M.H. Youssoufi, M. Mimouni, Z. H. Chohan, T. Ben Hadda, Petra, Osiris, and molinspiration together as a guide in drug design: predictions and correlation structure/antibacterial activity relationships of new N-sulfonyl monocyclic β -lactams, phosphorus. Sulfur, Silicon *Relat. Elem.* 185 (2010) 491–497, <https://doi.org/10.1080/10426500902953953>.
- [40] F. Cheng, W. Li, Y. Zhou, J. Shen, Z. Wu, G. Liu, P.W. Lee, Y. Tang, AdmetSAR: a comprehensive source and free tool for assessment of chemical ADMET properties, *J. Chem. Inf. Model.* 52 (2012) 3099–3105, <https://doi.org/10.1021/ci300367a>.
- [42] O. Trott, A.J. Olson, Software news and update AutoDock Vina: improving the speed and accuracy of docking with a new scoring function, efficient optimization, and multithreading, *J. Comput. Chem.* 31 (2010) 455–461, <https://doi.org/10.1002/jcc.21334>.

- [43] J.-H. Lin, Accommodating protein flexibility for structure-based drug design, *Curr. Top. Med. Chem.* 11 (2012) 171–178, <https://doi.org/10.2174/156802611794863580>.
- [44] F.R. Salsbury, Molecular dynamics simulations of protein dynamics and their relevance to drug discovery, *Curr. Opin. Pharmacol.* 10 (2010) 738–744, <https://doi.org/10.1016/j.coph.2010.09.016>.
- [45] N. Schmid, A.P. Eichenberger, A. Choutko, S. Riniker, M. Winger, A.E. Mark, W. F. Van Gunsteren, Definition and testing of the GROMOS force-field versions 54A7 and 54B7, *Eur. Biophys. J.* 40 (2011) 843–856, <https://doi.org/10.1007/s00249-011-0700-9>.
- [46] M.J. Abraham, T. Murtola, R. Schulz, S. Páll, J.C. Smith, B. Hess, E. Lindah, Gromacs: high performance molecular simulations through multi-level parallelism from laptops to supercomputers, *Software* 1–2 (2015) 19–25, <https://doi.org/10.1016/j.softx.2015.06.001>.
- [47] H.J.C. Berendsen, J.P.M. Postma, W.F. van Gunsteren, J. Hermans, Interaction models for water in relation to protein hydration, 1981, pp. 331–342, https://doi.org/10.1007/978-94-015-7658-1_21.
- [48] G. Bussi, D. Donadio, M. Parrinello, Canonical sampling through velocity rescaling, *J. Chem. Phys.* 126 (2007), <https://doi.org/10.1063/1.2408420>.
- [49] M. Parrinello, A. Rahman, Polymorphic transitions in single crystals: a new molecular dynamics method, *J. Appl. Phys.* 52 (1981) 7182–7190, <https://doi.org/10.1063/1.328693>.
- [50] B. Hess, H. Bekker, H.J.C. Berendsen, J.G.E.M. Fraaije, LINCS: a linear constraint solver for molecular simulations, *J. Comput. Chem.* 18 (1997) 1463–1472, [https://doi.org/10.1002/\(SICI\)1096-987X\(199709\)18:12<1463::AID-JCC4>3.0.CO;2-H](https://doi.org/10.1002/(SICI)1096-987X(199709)18:12<1463::AID-JCC4>3.0.CO;2-H).
- [51] U. Essmann, L. Perera, M.L. Berkowitz, T. Darden, H. Lee, L.G. Pedersen, A smooth particle mesh Ewald method, *J. Chem. Phys.* 103 (1995) 8577–8593, <https://doi.org/10.1063/1.470117>.
- [52] C. Huang, C. Li, P.Y.K. Choi, K. Nandakumar, L.W. Kostiuk, Effect of cut-off distance used in molecular dynamics simulations on fluid properties, *Mol. Simulat.* 36 (2010) 856–864, <https://doi.org/10.1080/08927022.2010.489556>.
- [53] R. Kumari, R. Kumar, O.S.D.D. Consortium, A. Lynn, g_mmpbsa - a GROMACS tool for MM-PBSA and its optimization for high-throughput binding energy calculations, *J. Chem. Inf. Model.* 54 (2014) 1951–1962.
- [54] S.K. Kwofie, E. Broni, J. Teye, E. Quansah, I. Issah, M.D. Wilson, W.A. Miller, E. K. Tiburu, J.H.K. Bonney, Pharmacoinformatics-based identification of potential bioactive compounds against Ebola virus protein VP24, *Comput. Biol. Med.* 113 (2019), <https://doi.org/10.1016/j.compbiomed.2019.103414>.
- [55] C. Suenderhuf, F. Hammann, J. Huwyler, Computational prediction of blood-brain barrier permeability using decision tree induction, *Molecules* 17 (2012) 10429–10445, <https://doi.org/10.3390/molecules170910429>.
- [56] S.J. Aditya Rao, P. Nandini Shetty, Evolutionary selectivity of amino acid is inspired from the enhanced structural stability and flexibility of the folded protein, *Life Sci* 281 (2021), 119774, <https://doi.org/10.1016/j.lfs.2021.119774>.
- [57] K. Yuki, M. Fujiogi, S. Koutsogiannaki, COVID-19 pathophysiology: a review, *Clin. Immunol.* 215 (2020), <https://doi.org/10.1016/j.clim.2020.108427>.
- [58] S.K. Miryala, S. Basu, A. Naha, R. Debroy, S. Ramaiah, A. Anbarasu, S. Natarajan, Identification of bioactive natural compounds as efficient inhibitors against Mycobacterium tuberculosis protein-targets: a molecular docking and molecular dynamics simulation study, *J. Mol. Liq.* 341 (2021), <https://doi.org/10.1016/j.molliq.2021.117340>.
- [59] M.T. Islam, C. Sarkar, D.M. El-Kersh, S. Jamaddar, S.J. Uddin, J.A. Shilpi, M. S. Mubarak, Natural products and their derivatives against coronavirus: a review of the non-clinical and pre-clinical data, *Phyther. Res.* 34 (2020) 2471–2492, <https://doi.org/10.1002/ptr.6700>.
- [60] K. Malathi, S. Ramaiah, Bioinformatics approaches for new drug discovery: a review, *Biotechnol. Genet. Eng. Rev.* 34 (2018) 243–260, <https://doi.org/10.1080/02648725.2018.1502984>.
- [61] J. Dyal, C.M. Coleman, B.J. Hart, T. Venkataraman, M.R. Holbrook, J. Kindrachuk, R.F. Johnson, G.G. Olinger, P.B. Jahrling, M. Laidlaw, L.M. Johansen, C.M. Lear-Rooney, P.J. Glass, L.E. Hensley, M.B. Frieman, Repurposing of clinically developed drugs for treatment of Middle East respiratory syndrome coronavirus infection, *Antimicrob. Agents Chemother.* 58 (2014) 4885–4893, <https://doi.org/10.1128/AAC.03036-14>.
- [62] H. Cao, Y. Zhang, J. Zhao, L. Zhu, Y. Wang, J. Li, Y.-M. Feng, N. Zhang, Prediction of the Ebola virus infection related human genes using protein-protein interaction network, *Comb. Chem. High Throughput Screen* 20 (2017), <https://doi.org/10.2174/1386207320666170310114816>.
- [63] N.J. Barrows, R.K. Campos, S.T. Powell, K.R. Prasanth, G. Schott-Lerner, R. Soto-Acosta, G. Galarza-Muñoz, E.L. McGrath, R. Urrabaz-Garza, J. Gao, P. Wu, R. Menon, G. Saade, I. Fernandez-Salas, S.L. Rossi, N. Vasilakis, A. Routh, S. S. Bradrick, M.A. Garcia-Blanco, A screen of FDA-approved drugs for inhibitors of Zika virus infection, *Cell Host Microbe* 20 (2016) 259–270, <https://doi.org/10.1016/j.chom.2016.07.004>.
- [64] K. Vasudevan, S. Basu, A. Arumugam, A. Naha, S. Ramaiah, A. Anbarasu, B. Veeraraghavan, Identification of potential carboxylic acid-containing drug candidate to design novel competitive NDM inhibitors: an in-silico approach comprising combined virtual screening and molecular dynamics simulation, *Res. Prepr.* (2021), <https://assets.researchsquare.com/files/rs-784343/v1/852884a0-692b-4972-8dc2-a63b773d8cc6.pdf?c=1637245347>.
- [65] M. Thillainayagam, S. Ramaiah, A. Anbarasu, Molecular docking and dynamics studies on novel benzene sulfonamide substituted pyrazole-pyrazoline analogues as potent inhibitors of Plasmodium falciparum Histone aspartic protease, *J. Biomol. Struct. Dyn.* 38 (2020) 3235–3245, <https://doi.org/10.1080/07391102.2019.1654923>.
- [66] M. Thillainayagam, K. Malathi, A. Anbarasu, H. Singh, R. Bahadur, S. Ramaiah, Insights on inhibition of Plasmodium falciparum plasmeprin I by novel epoxyazadiradione derivatives—molecular docking and comparative molecular field analysis, *J. Biomol. Struct. Dyn.* 37 (2019) 3168–3182, <https://doi.org/10.1080/07391102.2018.1510342>.
- [67] J. Gasteiger, T. Engel, *Chemoinformatics: A Textbook*, Wiley-VCH Verlag GmbH & Co. KGaA, 2003, <https://doi.org/10.1002/3527601643>.
- [68] P. Volarath, H. Wang, H. Fu, R. Harrison, Knowledge-based algorithms for chemical structure and property analysis, in: *Annu. Int. Conf. IEEE Eng. Med. Biol. - Proc.*, 2004, pp. 3011–3014, <https://doi.org/10.1109/iembs.2004.1403853>.
- [69] J.R. Ullmann, An algorithm for subgraph isomorphism, *J. ACM* 23 (1976) 31–42, <https://doi.org/10.1145/321921.321925>.
- [70] L.P. Cordella, P. Foggia, C. Sansone, M. Vento, Performance evaluation of the VF graph matching algorithm, in: *Proc. - Int. Conf. Image Anal. Process. ICIAP*, vol. 1999, 1999, pp. 1172–1177, <https://doi.org/10.1109/ICIAP.1999.797762>.
- [71] A. Prasansuklab, A. Theerasri, P. Rangsinth, C. Sillapachaiyaporn, S. Chuchawankul, T. Tencomnao, Anti-COVID-19 drug candidates: a review on potential biological activities of natural products in the management of new coronavirus infection, *J. Tradit. Complement. Med.* 11 (2021) 144–157, <https://doi.org/10.1016/j.jtcm.2020.12.001>.
- [72] J. Huang, G. Tao, J. Liu, J. Cai, Z. Huang, J.X. Chen, Current prevention of COVID-19: natural products and herbal medicine, *Front. Pharmacol.* 11 (2020), <https://doi.org/10.3389/fphar.2020.588508>.
- [73] A. Gamsi, S. Chirumbolo, M. Peana, S. Noor, A. Menzel, M. Dadar, G. Björklund, The role of diet and supplementation of natural products in COVID-19 prevention, *Biol. Trace Elem. Res.* (2021), <https://doi.org/10.1007/s12011-021-02623-3>.
- [74] R. Chakravarti, R. Singh, A. Ghosh, D. Dey, P. Sharma, R. Velayutham, S. Roy, D. Ghosh, A review on potential of natural products in the management of COVID-19, *RSC Adv* 11 (2021) 16711–16735, <https://doi.org/10.1039/d1ra00644d>.